Enhanced photocatalytic degradation of methyl violet using nanoporous Niobium oxide ceramics.

[a*]Shaik Jaheer Basha, [b] B.Yagna Narayana [c] Sarika.G

[a*, c] Department of Humanities and Sciences, Annamacharya Institute of Technology and Sciences, Kadapa Andhra Pradesh state-516003, India.

[b] Department of Humanities and Sciences, Annamacharya Institute of Technology and Sciences, Tirupati, Andhra Pradesh state-517520, India.

Abstract- *A nanoporous composite ceramic material was created through the sol-gel process and successfully incorporated with a nanoporous structure. The NbO nanocomposite was successfully synthesized using a simple chemical reduction technique. The activated Porous carbons made with colloidal SiO_2 crystals as models organized three-dimensional interconnected pores via a Sol-Gel matrix. X-ray photoelectron spectroscopy (XPS), UV-Vis absorbance, diffuse reflectance spectra (UV-DRS), FT-Raman, X-ray diffraction (XRD), Surface-enhanced Raman scattering (SERS), CV, FT-IR, and high resolution-transmission electron microscopy (HR-TEM) have been used to characterize synthesized Nbo nanocomposite. These results are utilized to analyze the structure, size, and interactions of the nanostructure. Theoretical calculations and photodegradation studies on methyl violet are studied for systems.*

Keywords: NbO, porous nanocomposites, methyl violet, photodegradation, SERS, XPS.

1. INTRODUCTION

The use of nanoparticles has been widespread in various industries, including cosmetics, ceramics, electronics, optics, and biology. When compared to elements in their natural states, nanoparticles have a much broader range of applications. This article will delve into the properties and applications of niobium oxide nanoparticles. The Niobium Pentoxide (Nb_2O_5) is an n-type semiconductor with a lower band gap (3.4 eV) than other metal oxides. It is interesting to study Nb_2O_5 because of its outstanding physicochemical properties and structural isotropy, which make it suitable for a wide range of applications such as electrochromic displays, gas sensing, and photo electrodes, as well as field-emission displays and microelectronics[1-6]. Earlier studies on the use of Nb_2O_5 nanoparticles for cleaning the environment in water for photocatalytic processes were carried out. Nb_2O_5 nanocomposite exhibits high potential in these photocatalytic approaches because of its aqueous medium consistency, surface activity, redox, and photocatalytic capabilities that are fundamentally linked to its structure [7-9]. At low temperatures, the primary crystalline phases documented in journals for Nb_2O_5 include TT-Nb_2O_5 (pseudohexagonal), T-Nb_2O_5 (orthorhombic structure) heating to 600 and 800°C, and H- Nb_2O_5 (monoclinic structure) heating to around 1100°C. The initial materials, synthesis process, and heat treatment conditions are the main factors that determine the crystallization phase of each Nb_2O_5 structure. Among the numerous niobium oxides, including NbO, NbO_2, and Nb_2O_5, niobium-pentoxide (Nb_2O_5) is the most thermodynamically stable form [10]. This material is extensively used in catalysts, gas-sensing applications, and optical filters[11-14]. Previous research studies have shown that nanoporous Nb_2O_5 is a feasible electrochromic material with significant intercalation properties. The higher surface-to-volume ratio, shape, and very small size have all contributed to metal nanocomposite's efficiency as a catalyst [15-17].

2. Experimental section

2.1. Materials

Niobium pentoxide (99%, Sigma Aldrich), 3-aminopropyltriethoxysilane (APTES-98.0%), and other reagents and solvents were obtained from HiMedia Laboratories Pvt. Ltd. (Mumbai, India), and tetraethoxysilane (TEOS, 98.0%, Alfa Aesar) was used without additional purification. All of the aqueous solutions were made with nano-pure water. All apparatus and glassware were cleaned with acetone, rinsed with deionized water (DIW), and dried in an air-hot oven at 100 °C before being utilized in the investigations.

2.2. Synthesis of Nb_2O_5 doped amine-functionalized silica nanocomposite powder (Nb_2O_5@SiO_2 nanocomposites)

Nb_2O_5@SiO_2 nanocomposite was synthesized by the sol-gel chemical route. Figure 1 depicts the synthetic route of Nb_2O_5@SiO_2 nanocomposite. Briefly, TEOS (3 mL) and APTES (1 mL) were dissolved in distilled ethanol (3 mL) in a shielded beaker and stirred for 30 min at the temperature range of 40–45 °C. Meanwhile, 0.01M of Nb_2O_5 (3 mL) was added to the reaction mixture. This mixture was stirred for another 30 min at room temperature to form the Nb_2O_5@SiO_2 sol-gel mixture.

Then, the sol-gel mixture was placed in a hot-air oven for 12 hrs at 100 °C for aging, drying, and shrinking. The obtained zero-gel matrix was ground well to obtain a final form of $Nb_2O_5@SiO_2$ nanocomposite powder.

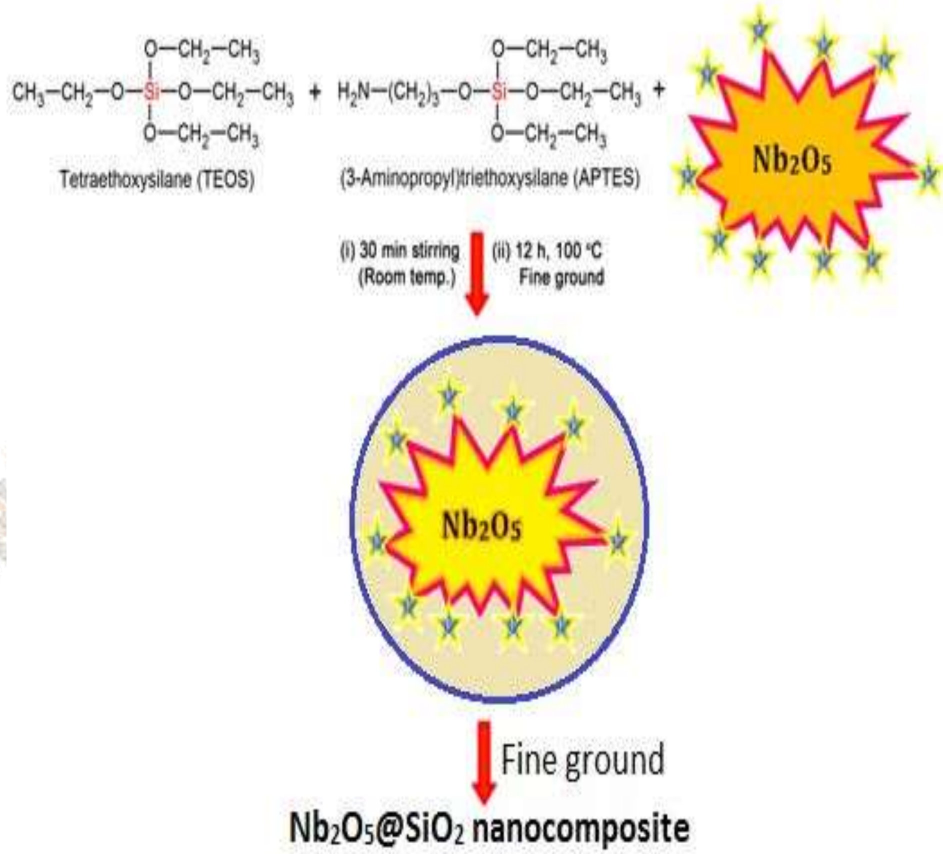

Fig 1. Synthesis of Nb_2O_5 doped amine-functionalized silica nanocomposite powder

($Nb_2O_5@SiO_2$ nanocomposites)

2.3 X-ray Diffractions

The diffraction pattern of Nb_2O_5 is presented in **Fig.2**, the planes are identified and compared with JCPDS data in **Table 1**.

2.4 FT-IR analysis

The following **Fig.3** represents the FT-IR of synthesized Nb_2O_5 nanoparticles, representing the characteristic peaks. FT-IR analysis identifies the functional groups which are bounded characteristically for the formation of Nb_2O_5. The strong peak of absorption bond at 3040.11 cm^{-1} corresponds to a hydroxyl group (-O-H) stretching vibration this is due to water presence. The peak at 2303.25 cm^{-1} represents alkenes (-C=C-) stretching vibration.

The peak at 2115.05 cm^{-1} represents C=C stretching vibrations. Another highly intense peak at 1066 cm^{-1} is absorbed due to C=O. In 1996 cm^{-1} stretching vibrations represented C-N bonds. At 790.50 cm^{-1} and 638.9 cm^{-1} representing the presence of Niobium oxide out of bending vibrations.

FT-IR spectroscopy was used to characterize and identify the chemical composition of the AgNP surface. The FT-IR spectra of control dried tea extract (before reaction without $AgNO_3$) and synthesized AgNPs (after reaction with $AgNO_3$) are shown in Fig.3. Both of them showed a shift in peaks: 3420–3371 (due to N–H stretching, amides), 2931–2925 (due to C–H stretching, alkanes), 1383–1371 (characteristic of hydroxyl groups, phenolic hydroxyl), 1051–1044 cm^{-1} (due to C-stretching, ether groups). In addition, the synthesized AgNPs showed other peaks at 1695, 1452, 1241, and 926 cm^{-1} related to alkene groups (C═C stretching), tertiary ammonium ions, poly phenols, aliphatic amines (C–N stretching vibrations), and alkene groups (C–H stretching), respectively. The FT-IR analysis indicated the involvement of amides, carboxyl, amino groups, and polyphenols in the synthesized AgNPs. It is well known that there are tea polyphenols, proteins, and amino acids in tea. The organic compounds in tea extract could attribute to the reduction of $AgNO_3$ and the stabilization of AgNPs by the surface-bound organic compounds.

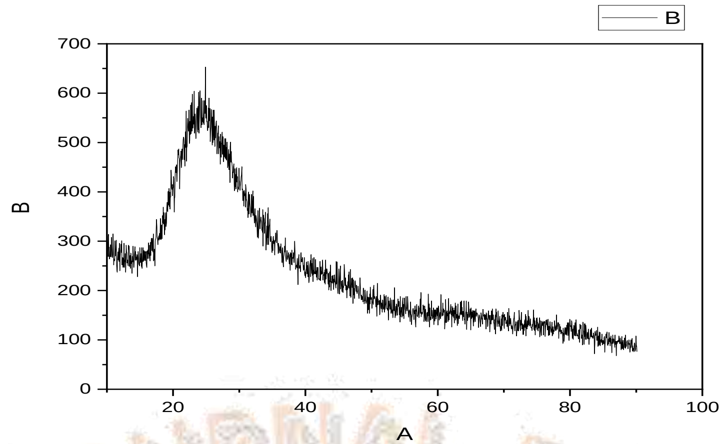

Fig 2. X-ray Diffraction pattern

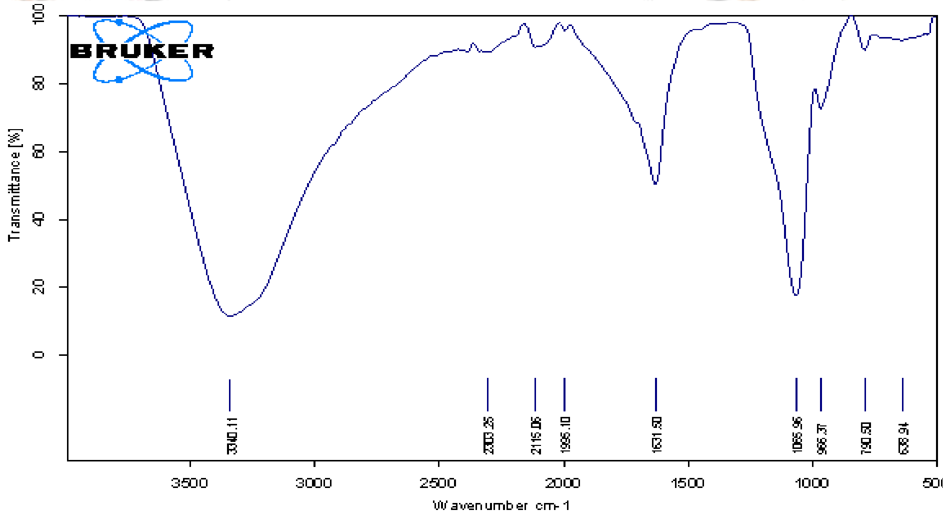

Fig 3. FT-IR of synthesized Nb_2O_5 nanoparticles

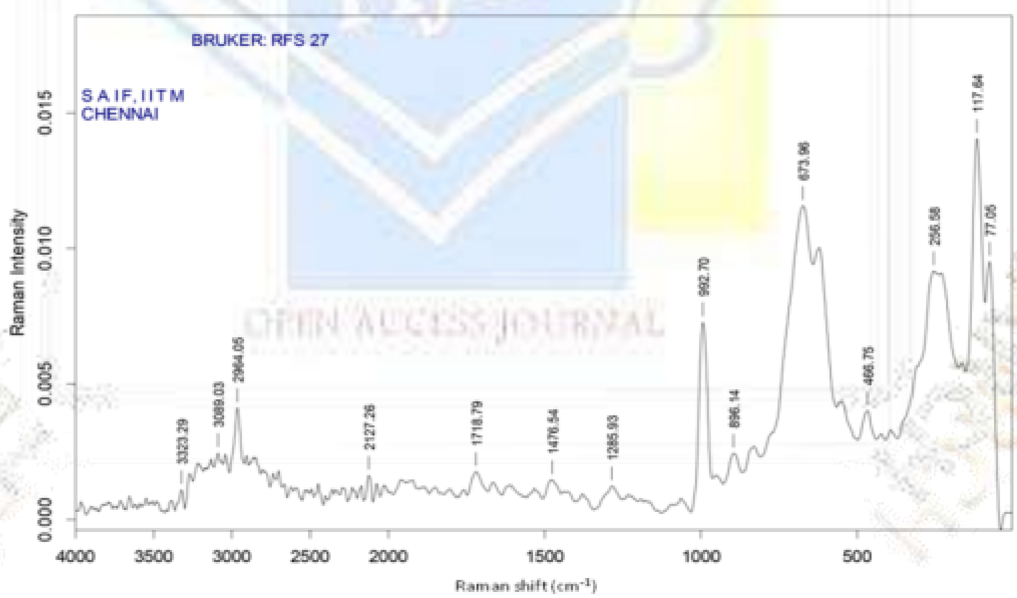

Fig 4. FT-Raman Spectroscopy

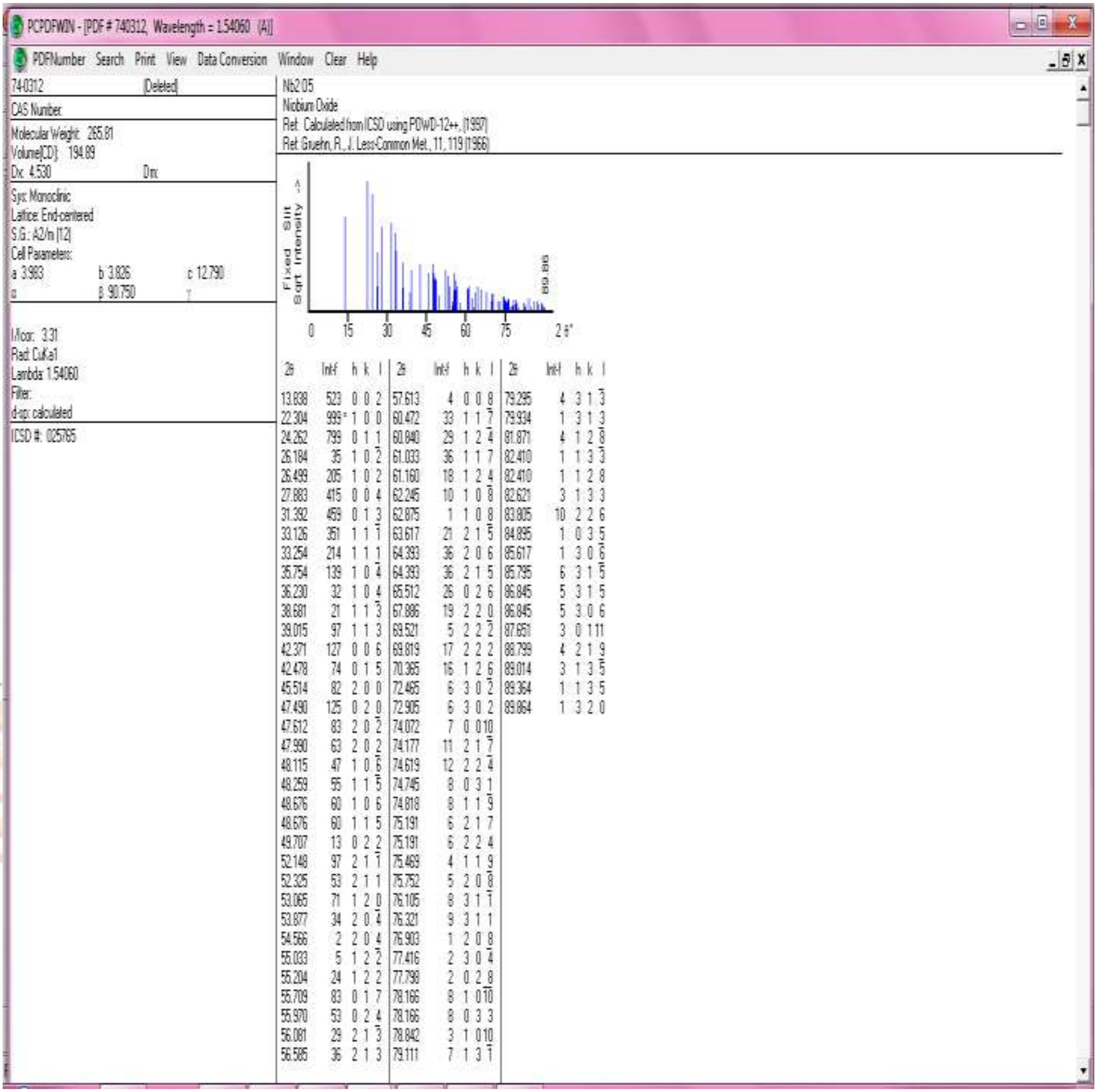

2θ	Int-f	h	k	l	2θ	Int-f	h	k	l	2θ	Int-f	h	k	l
13.838	523	0	0	2	57.613	4	0	0	8	79.295	4	3	1	$\bar{3}$
22.304	999*	1	0	0	60.472	33	1	1	$\bar{7}$	79.934	1	3	1	3
24.262	799	0	1	1	60.840	29	1	2	$\bar{4}$	81.871	4	1	2	$\bar{8}$
26.184	35	1	0	$\bar{2}$	61.033	36	1	1	7	82.410	1	1	3	$\bar{3}$
26.499	205	1	0	2	61.160	18	1	2	4	82.410	1	1	2	8
27.883	415	0	0	4	62.245	10	1	0	$\bar{8}$	82.621	3	1	3	3
31.392	459	0	1	3	62.875	1	1	0	8	83.805	10	2	2	6
33.126	351	1	1	$\bar{1}$	63.617	21	2	1	$\bar{5}$	84.895	1	0	3	5
33.254	214	1	1	1	64.393	36	2	0	6	85.617	1	3	0	$\bar{6}$
35.754	139	1	0	$\bar{4}$	64.393	36	2	1	5	85.795	6	3	1	$\bar{5}$
36.230	32	1	0	4	65.512	26	0	2	6	86.845	5	3	1	5
38.681	21	1	1	$\bar{3}$	67.886	19	2	2	0	86.845	5	3	0	6
39.015	97	1	1	3	69.521	5	2	2	$\bar{2}$	87.651	3	0	1	11
42.371	127	0	0	6	69.819	17	2	2	2	88.799	4	2	1	9
42.478	74	0	1	5	70.365	16	1	2	6	89.014	3	1	3	$\bar{5}$
45.514	82	2	0	0	72.465	6	3	0	$\bar{2}$	89.364	1	1	3	5
47.490	125	0	2	0	72.905	6	3	0	2	89.864	1	3	2	0
47.612	83	2	0	$\bar{2}$	74.072	7	0	0	10					
47.990	63	2	0	2	74.177	11	2	1	$\bar{7}$					
48.115	47	1	0	$\bar{6}$	74.619	12	2	2	$\bar{4}$					
48.259	55	1	1	$\bar{5}$	74.745	8	0	3	1					
48.676	60	1	0	6	74.818	8	1	1	$\bar{9}$					
48.676	60	1	1	5	75.191	6	2	1	7					
49.707	13	0	2	2	75.191	6	2	2	4					
52.148	97	2	1	$\bar{1}$	75.469	4	1	1	9					
52.325	53	2	1	1	75.752	5	2	0	$\bar{8}$					
53.065	71	1	2	0	76.105	8	3	1	$\bar{1}$					
53.877	34	2	0	$\bar{4}$	76.321	9	3	1	1					
54.566	2	2	0	4	76.903	1	2	0	8					
55.033	5	1	2	$\bar{2}$	77.416	2	3	0	$\bar{4}$					
55.204	24	1	2	2	77.798	2	0	2	8					
55.709	83	0	1	7	78.166	8	1	0	$\bar{10}$					
55.970	53	0	2	4	78.166	8	0	3	3					
56.081	29	2	1	$\bar{3}$	78.842	3	1	0	10					
56.585	36	2	1	3	79.111	7	1	3	$\bar{1}$					

Table 1. JCPDS data of Nb_2O_5

2.5 RAMAN /SERS Spectra

Raman spectra are used to support information on XRD conformations of structure and corresponding vibration band assignments[18-20]. Raman spectroscopy was applied to determine the relationship between niobium pentaoxide structures and their corresponding Raman spectra. The assignments of the Raman bands were based on the known Niobium pentoxide structures. The Raman studies indicate that the Raman frequencies strongly depend on the Niobium pentoxide structures. For the slightly distorted octahedral NbO_6 structures ($KNbO_3$, $NaNbO_3$, and $LiNbO_3$), the major Raman frequencies appear in the 500-700 cm^{-1} region. For the highly distorted octahedral NbO_6 structures ($K8Nb_6O_{19}$, $AlNbO_4$, and $Nb(HC_2O_4)_5$), the major Raman frequencies shift from 500-700 to 850-1000 cm^{-1} region. Figure 4 shows detailed Raman spectroscopy, which provides structural details of Nb_2O_5 nano composite whether it is hydrated, dehydrated (crystalline), or crystalline phases of Nb_2O_5 nanocomposite. Niobium pentoxide of nanocomposite of Raman spectra shows broad speaks at ∼256 cm^{-1}, ∼673cm^{-1}, ∼ 466.75 $cm^{-1,}$ ∼896 $cm^{-1,}$ and ∼992.70 cm^{-1} which are related to Nb-O-Nb symmetric and bending modes vibrations, conformed that presence of Nb-O-Nb bonds from spectra.

2.6 TEM Micrograph

The following **Fig. 5** shows the synthesized Nb_2O_5 nanoparticles in transmission electron microscopy (TEM). TEM analysis was performed for a more detailed study of the morphology and size of Nb_2O_5 nanocomposite, TEM is a high-resolution tool, able to analyze at high resolution at a nano level. TEM is used to measure nanoparticles size, measurement of grain size, crystallite size, atomic arrangement in material, and formation of new phases with a very low amount which cannot detect by XRD, by using TEM we can detect low amount (<10 %) phases.

The typical TEM image of the nanospheres can be seen that the nanosphere is about 10–50nm in length and agglomeration with sphere nanoparticles. Agglomeration is due to moisture presence.

2.7 SEM Micrograph

Scanning electron microscopy (SEM) studies were performed on the samples to reveal surface features of Niobium Penta oxide, the SEM/EDAX studies were performed generally for material identification. They were done in an ultra-high-vacuum system with a base pressure of about 146.65×10^{-6} Pa. The EDS survey was done to present the general composition of the nanocomposite, The measurements were performed using an eXplorer VP, Model 8831 of ASPEX Corporation with the software Aspex Corporation Perception Console v. 3.0.393. The following **Fig.6**, SEM Image shows that the niobium composite particle seems to be agglomeration due to moisture present in the samples.

3. Degradation of Methyl Violet dye

The catalytic activity of synthesized niobium oxide nanocomposite was performed by degrading the methyl violet dye. To reduce the methyl violet dye, 5 mg/L of niobium nanocomposite purified was added to the 10 mg/L of crystal violet solution. This solution was exposed to UV light at the range of 365 nm in a photo reactor. The photocatalytic capacity of niobium oxide nanocomposite was monitored by UV–vis spectrophotometer at 30 min time intervals, methyl violet dye is degraded as shown in **Fig.7**, and also concerning niobium oxide nanoparticles UV-Vis spectrum is plotted in **Fig.8**.

4. Conclusions

In summary, Nb_2O_5 nanoporous composite ceramic material has been successfully fabricated by the sol-gel method, The synthesized NbO nanocomposite is characterized by UV-Vis, FT-IR, SERS, XRD, and HR-TEM techniques. The results were used to examine the morphologies, size of the nanostructure, and its interactions. The theoretical calculation and photodegradation studies of methyl violet were studied.

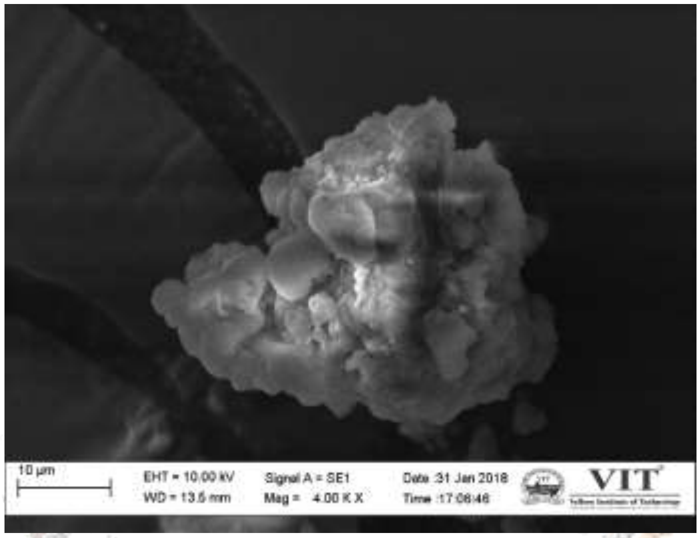

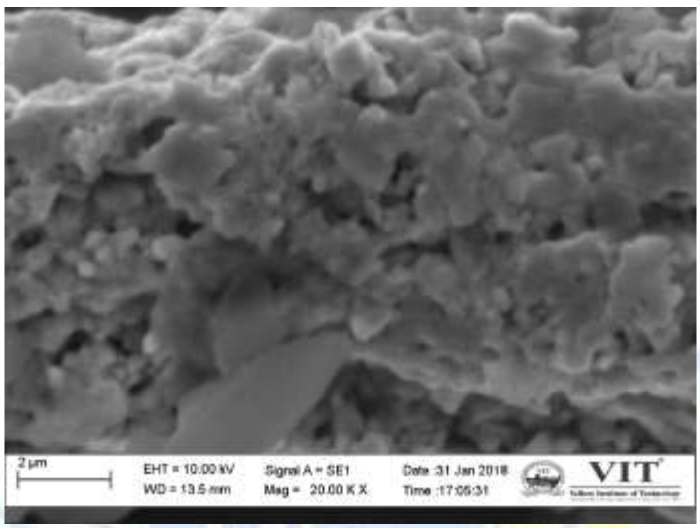

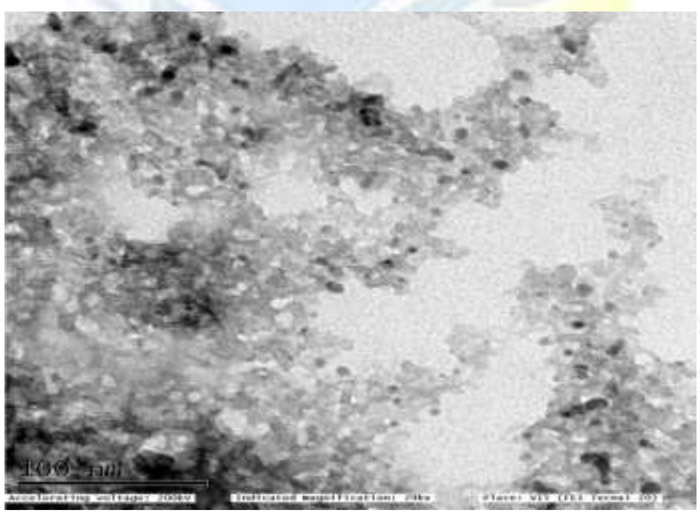

Fig 5. TEM of Nb_2O_5 nanoparticles

Spectrum processing: Nb1

No peaks omitted

Processing option: All elements analyzed (Normalized)

Number of iterations = 4

Standard :

C $CaCO_3$ 1-Jun-1999 12:00 AM

O SiO_2 1-Jun-1999 12:00 AM

Si SiO_2 1-Jun-1999 12:00 AM

Nb Nb 1-Jun-1999 12:00 AM

Element	Weight (%)	Atomic (%)
C K	43.05	54.21
O K	39.34	37.19
Si K	15.25	8.21
Nb L	2.37	0.39
Total	100.00	

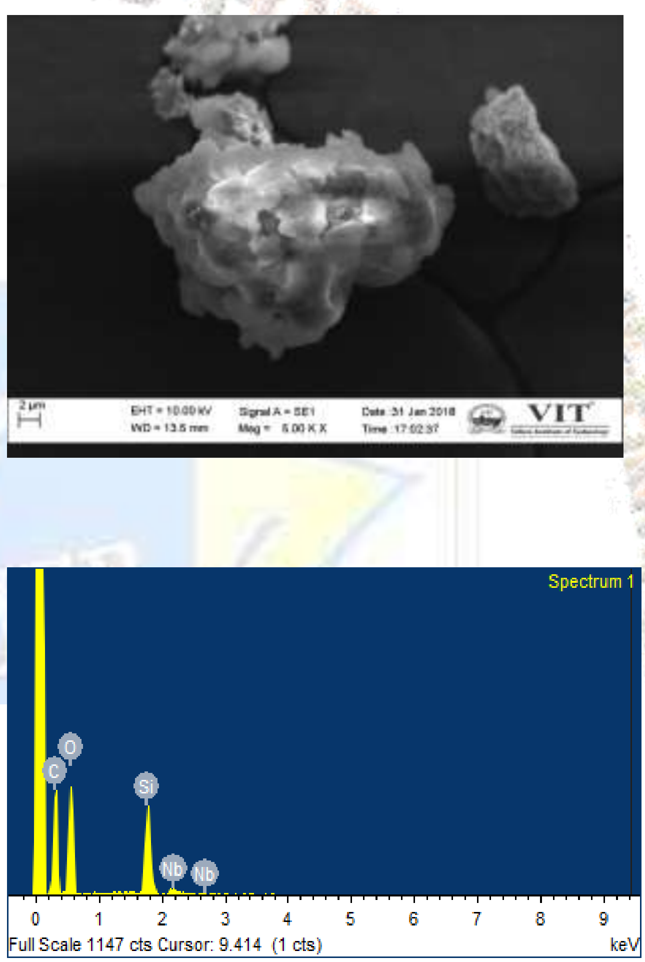

Fig 6. SEM & EDAX of Nb_2O_5 Nano particles

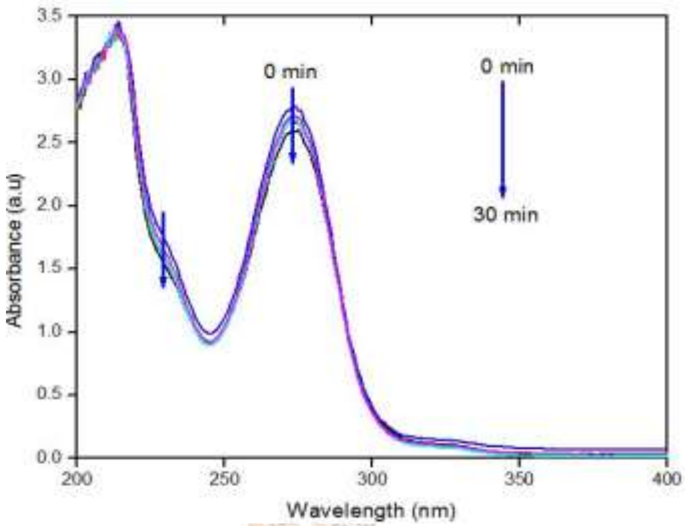

Fig.7 Degradation of Methyl Violet dye

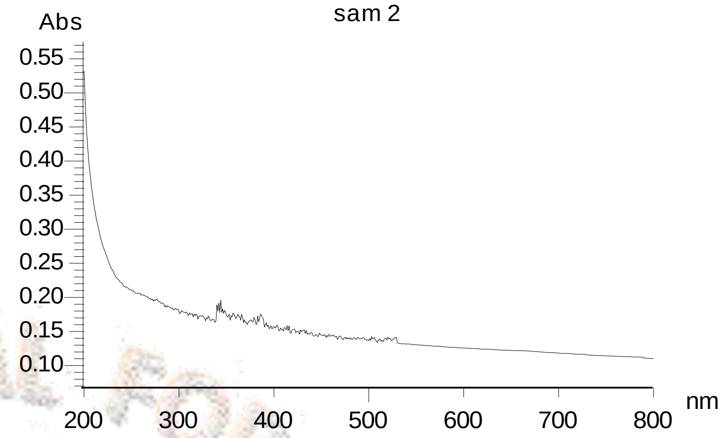

Fig.8 UV-Vis of Niobium Oxide Nanoparticles

References

[1].Wang YD, Yang LF, Zhou ZL, Li YF, Wu XH, " Effects of calcining temperature on lattice constants and gas-sensing properties of Nb_2O_5 ", *Materials Letters*, Vol 49(5), pp.277-281, July 2001.

[2].Mujawar S.H, Inamdar A.I, Patil S.B, Patil P.S, " Electrochromic properties of spray-deposited niobium oxide thin films", *Solid State IonicsI,* Vol 177 (37-38), pp.3333-3338, December 2006.

[3].Jose R, Thavasi V, Ramakrishna S, "Metal Oxides for Dye-Sensitized Solar Cells", *Journal of the American Chemical Society*, Vol 92(2), pp.289-301, February 2009.

[4].Lira-Cantu M, Krebs FC," Hybrid solar cells based on MEH-PPV and thin film semiconductor oxides (TiO_2, Nb_2O_5, ZnO, CeO_2 and CeO_2 –TiO_2): Performance improvement during long-time irradiation", *Solar Energy Materials and Solar Cells*, Vol 90 (14), pp.2076-2086, September 2006.

[5].Ahn KS, Kang MS, Lee JK, Shin BC, Lee JW, " Enhanced electron diffusion length of mesoporous TiO2 film by using Nb_2O_5 energy barrier for dye-sensitized solar cells", *Applied Physics Letters*, Vol 89, pp.013103, July 2006.

[6]. Hashemzadeh F, Gaffarimejad A, Rahimi R, "Porous p-NiO/n-Nb_2O_5 nanocomposites prepared by an EISA route with enhanced photocatalytic activity in simultaneous Cr(VI) reduction and methyl orange decoloration under visible light irradiation", *Journal of Hazardous Materials*. Vol 286, pp.64-74, April 2015.

[7].Carniti P, Gervasini A, Marzo M, "Dispersed NbO_x Catalytic Phases in Silica Matrixes: Influence of Niobium Concentration and Preparative Route", *The Journal of Physical Chemistry C*, Vol.112, pp.14064-14074, August 2008.

[8]. Sreethawong T, Ngamsinlapasathian S, Lim SH, Yoshikawa S, "Investigation of thermal treatment effect on physicochemical and photocatalytic H2 production properties of mesoporous-assembled Nb_2O_5 nanoparticles synthesized via a surfactant-modified sol–gel method", *Chemical Engineering Journal*.Vol 215-216, pp.322-330, January 2013.

[9]. Marin ML, Hallett-Tapley GL, Impellizzeri S, Fasciani C, Simoncelli S, Netto-Ferreira JC, and Scaiano J.C, " Synthesis, acid properties and catalysis by niobium oxide nanostructured materials", *Catalysis Science & Technology*, Vol. 4, pp.3044-3052, April 2014.

[10]. Venkata Raju S, Drese R, Liesch Ch, Kappertz O, Jayavel R, Wuttig M, "Temperature stability of sputtered niobium-oxide films", *Journal of Applied Physics*, Vol.91, pp.4863, March 2002.

[11].Sieber I, Hilderbrand H, Friedrich A, Schmuki P, " Formation of self-organized niobium porous oxide on niobium", *Electrochemistry Communications*, Vol.7, pp.97-100, January 2005.

[12].Gimon-Kinsel M.E and Balkus Jr K.J, " Pulsed laser deposition of mesoporous niobium oxide thin films and application as chemical sensors", *Micropororous Mesopororous Materials,* Vol.28(1), pp.113-123, March 1999.

[13].Özer N, Chen D.G, Lampert Carl M, " Preparation and properties of spin-coated Nb_2O_5 films by the sol-gel process for electrochromic applications", *Thin solid films,* Vol.277, pp.162-168, August 1996.

[14].Viswanathamurthi P, Bhattarai N, Kim H.Y, Lee D.R, Kim S.R, Morris M.A, " Preparation and morphology of niobium oxide fibers by electrospinning", *Chemical Physics Letters*, Vol.374 (1-2), pp.79-84, June 2003.

[15]. Siby J, Beena M, "Microwave-assisted green synthesis of silver nanoparticles and the study on catalytic activity in the degradation of dyes", Journal of Molecular Liquids, Vol.204, pp.184-191, Apr 2015.

[16].Roopan S.M, Ganesh E, "Exploitation of Cocos nucifera a non-food toward the biological and nanobiotechnology field", *Industrial Crops and Products,* Vol.67, pp.130-136, May 2015.

[17].Hemalatha K, Madhumitha G, "Eco-friendly synthesis of palladium nanoparticles, environmental toxicity assessment and its catalytic application in Suzuki Miyaura Coupling", *Research Journal of Pharmacy and Technology*, Vol.8(12), pp.1691-1700, December 2015.

[18].Govindhan R, Karthikeyan B, "Nano copper interaction with single amino acid tyrosine derived self-assemblies; study through XRD, AFM, confocal Raman microscopy, SERS and DFT methods", *Journal of Physics and Chemistry of Solids*, Vol.111, pp. 123-134, December 2017.

[19].Yamada H, Tagawa K, Komatsu M, Moriguchi I, Kudo T, "High power battery electrodes using nanoporousV_2O_5Carbon composites", *Journal of Physical Chemistry C*, Vol.111(23), 8397-8402, May 2017.

[20].Govindhan R, Karthikeyan B, "XRD and spectral dataset of the UV-A stable nanotubes of 3,5-bis(trifluoromethyl)benzylamine derivate of tyrosine, *Data in Brief*, Vol.14, pp.579-583, October 2017.